ChemPubSoc Europe

DOI: 10.1002/cctc.201500065

CHEMCATCHEM Full Papers

Rhodium Nanoparticles as Precursors for the Preparation of an Efficient and Recyclable Hydroformylation Catalyst

Marco A. S. Garcia,[a] Kelley C. B. Oliveira,[b] Jean C. S. Costa,[a] Paola Corio,[a] Elena V. Gusevskaya,[b] Eduardo N. dos Santos,[b] and Liane M. Rossi*[a]

Despite all the advances in the application of nanoparticle (NP) catalysts, they have received little attention in relation to the hydroformylation reaction. Herein, we present the preparation of a hydroformylation catalyst through the immobilization of air-stable rhodium NPs onto a magnetic support functionalized with chelating phosphine ligands, which serves as an alternative to air-sensitive precursors. The catalyst was active in hydroformylation and could be used in successive reactions with negligible metal leaching. The interaction between the rhodium NPs and the diphenylphosphine ligand was evidenced by an enhancement in the Raman spectrum of the ligand. Changes occurred in the Raman spectrum of the catalyst recovered after the reaction, which suggests that the rhodium NPs are precursors of active molecular species that are formed in situ. The supported catalyst was active for successive reactions even after it was exposed to air during the recycling runs and was easily recovered through magnetic separation.

Introduction

Aldehydes are valuable final products and intermediates in the synthesis of bulk chemicals such as alcohols, esters, and amines. They can be accessed by the hydroformylation of olefins, one of the most important homogeneously catalyzed reactions in the industry.[1] Large-scale cobalt- and rhodium-based processes are mature technologies; however, the hydroformylation reaction has been less explored for the production of fine chemicals.[2] The reasons for this relate not only to catalytic activity, chemo- and regioselectivity, and stability but also to important safety issues in working with carbon monoxide, which is toxic, and to its high cost at present. Alternative syngas sources, such as gasification of biomass, will stimulate the production of valuable chemicals from this renewable feedstock in the near future.

The search for more stable ligands and more active and regioselective catalytic systems for hydroformylation has been the focus of intense research.[3] Theoretically, the hydroformylation reaction can produce aldehydes with 100% atom economy; however, parallel side reactions such as carbon–carbon double bond isomerization and hydrogenation often decrease the selectivity towards target products. The use of rhodium complexes with ancillary phosphorus ligands can usually provide high reaction rates and selectivity in hydroformylation reactions.[4] These reactions mostly occur as homogeneous processes in which the separation of the catalyst from the reaction medium is time-consuming and requires a significant effort to guarantee product purification and metal recovery. In this context, the heterogenization of homogeneous catalysts[5] and the use of metal nanoparticles (NPs) as catalysts[6] have been considered as alternatives to overcome the drawbacks of homogeneous catalytic systems in hydroformylation processes.

Many attempts have been made to anchor metal complexes to solid supports to improve their stability and enable their reuse in successive reactions. The most common supports used are silica,[7] clays,[8] and active carbon,[9] although other materials have also been tested.[10] Only a few papers have been published on the immobilization of rhodium NPs on solid supports such as silica,[6f,11] carbon,[6c] and hypercrosslinked polystyrene.[12] In most cases, no experimental proof that the hydroformylation reaction occurs on the surface of metal NPs has been provided. Alternatively, the NPs can serve as reservoirs for the active molecular rhodium species formed by metal leaching into the solution owing to the interaction with auxiliary phosphorus ligands and/or carbon monoxide.[6b]

Herein, we present the preparation of a magnetically recoverable and reusable hydroformylation catalyst through the immobilization of rhodium NPs stabilized with tetraoctylammonium bromide (Rh-TOAB NPs) on a magnetic support with the surface functionalized with propylamino bis(methylenediphenylphosphine) ligands. The active species are formed in situ and are maintained on the magnetic support surface after magnetic separation. Recycling studies show negligible metal leaching and high activity in successive reactions.

[a] M. A. S. Garcia, Dr. J. C. S. Costa, Dr. P. Corio, Dr. L. M. Rossi
Institute of Chemistry
University of São Paulo
Av. Prof. Lineu Prestes, 748, 05508-000 São Paulo (Brazil)
E-mail: lrossi@iq.usp.br

[b] Dr. K. C. B. Oliveira, Dr. E. V. Gusevskaya, Dr. E. N. dos Santos
Chemistry Department
Federal University of Minas Gerais
Av. Antônio Carlos, 6627, 31270-901 Belo Horizonte (Brazil)

Results and Discussion

We have previously reported that Rh-TOAB NPs (colloidal solution or after their immobilization in an amino-functionalized silica-coated magnetite support (Fe_3O_4@SiO_2-NH_2Rh)) are active catalysts for the solventless hydrogenation of cyclohexene.[16] The Fe_3O_4@SiO_2-NH_2Rh material is attractive because it can be easily recovered after the reaction for reuse. The colloidal Rh-TOAB NPs and the supported NPs were both tested in the hydroformylation of oct-1-ene (**1a**) in toluene solutions (Table 1).

Rh-TOAB NPs slowly converted **1a** at 80 °C, which mainly resulted in hydroformylation products—aldehydes **1b** and **c** (Scheme 1; Table 1, run 1). At 120 °C, the reaction occurred quickly and was completed in 21 h (Table 1, run 2). A pronounced induction period was observed because for the first 6 h, no substrate conversion was detected. The considerable amounts of other aldehydes among the products (≈30%) indicated that Rh-TOAB NPs or their fragments also promoted the extensive isomerization of **1a** and further hydroformylation of its internal isomers. Minor products presented in Table 1 as "other aldehydes" and "alcohols" were attributed to unidentified aldehydes and alcohols owing to characteristic GC retention times and the presence of characteristic peaks in their mass spectra.

Although Rh-TOAB NPs promote the hydroformylation of **1a**, their recovery from colloidal reaction mixtures is difficult and makes their practical use less attractive. In an attempt to obtain a solid and magnetically recoverable catalyst, we tested in the hydroformylation of **1a** the Fe_3O_4@SiO_2-NH_2Rh material composed of rhodium NPs immobilized on the amino-functionalized support (Table 1, runs 2 and 3). The Fe_3O_4@SiO_2-NH_2Rh catalyst quickly converted the substrate into the hydroformylation products even at 80 °C, which showed a 100% conversion in 6 h. Notably, no appreciable substrate hydrogenation occurred with either solid Fe_3O_4@SiO_2-NH_2Rh or colloidal Rh-TOAB NPs. After the reactions in runs 3 and 4 (Table 1), the catalyst was removed magnetically by placing a permanent magnet on the reactor wall; then, a portion of fresh **1a** was added and the reactions were allowed to proceed further (Table 1, runs 5 and 6). In both runs, the supernatants promoted a complete substrate conversion in 6 h. Furthermore, the inductively coupled plasma optical emission spectrometry (ICP–OES) analysis confirmed that approximately 80% of the initial rhodium leached from the solid material into the solution during the first use of the catalyst. Moreover, the spent Fe_3O_4@SiO_2-NH_2Rh material recovered after the first reaction showed no activity in a recycling run (Table 1, run 7).

Table 1. Hydroformylation of **1a** catalyzed by Rh-TOAB NPs and Fe_3O_4@SiO_2-NH_2Rh.[a]

Run	Catalyst	T [°C]	T [h]	Conversion [%]	Selectivity [%]			
					Aldehydes			Alcohols
					1b	1c	Other	
1	Rh-TOAB	80	21	5	30	70	–	–
2	Rh-TOAB	120	6	0	–	–	–	–
			21	100	35	36	26	3
3	Fe_3O_4@SiO_2-NH_2Rh	120	6	100	38	28	20	13
4	Fe_3O_4@SiO_2-NH_2Rh	80	6	100	42	32	12	13
5[b]	supernatant after run 3	120	6	100	36	30	20	14
6[b]	supernatant after run 3	80	6	100	47	33	12	9
7[c]	Fe_3O_4@SiO_2-NH_2Rh	80	6	0	–	–	–	–

[a] Reaction conditions: **1a** (2 mmol), catalyst (3.4 μmol of Rh: 3.6 mL of the 28 ppm solution of Rh-TOAB in toluene or 50 mg of Fe_3O_4@SiO_2-NH_2Rh), toluene (up to total volume of 10 mL), P = 60 atm (CO/H_2 = 1); conversion and selectivity were determined from GC analysis; difference in mass balance (if any) refers to double bond isomerization products; [b] After runs 3 and 4, the catalyst was magnetically removed, fresh **1a** (2 mmol) added, and the reaction allowed to proceed; [c] The spent catalyst recycled after run 4 was used in this run.

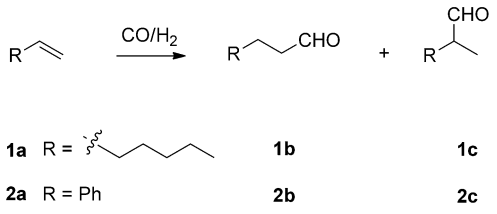

Scheme 1. Hydroformylation of **1a** and **2a**.

Although the Fe_3O_4@SiO_2-NH_2Rh material is active in hydroformylation, it does not present metal–support interactions strong enough to immobilize rhodium on the surface under hydroformylation conditions and essentially loses the metal to the reaction solutions. Our further efforts were directed towards the development of another Fe_3O_4@SiO_2-based support, which would be functionalized adequately to maintain rhodium under conventional hydroformylation conditions and to prevent metal leaching. Silica-coated magnetic NPs (Fe_3O_4@SiO_2) are an attractive support for catalytically active species, because they can be uniformly attracted to a permanent magnet and completely separated from reaction solutions through this simple procedure.[17]

The silica surface can be functionalized with various ligands using commercially available alkoxyorganosilanes [$(OR')_3Si(CH_2)_3$-R, R = NH_2, Cl, SH, etc., and R' = Et, Me] or compounds derived from them by means of various reactions such as amine alkylation. It is expected that the presence of functional groups grafted on the support surface can improve the impregnation of NPs, which can not only increase the metal uptake[18] but also affect the catalytic performance of NPs.[19] The silica support functionalized with aminopropyl groups (Fe_3O_4@SiO_2-NH_2) was used to further functionalize the support with an organic moiety bearing a terminal phosphine group (Scheme 2). The phosphine moieties were introduced through the reaction of terminal amino groups grafted on the support surface with paraformaldehyde and diphenylphosphine. The

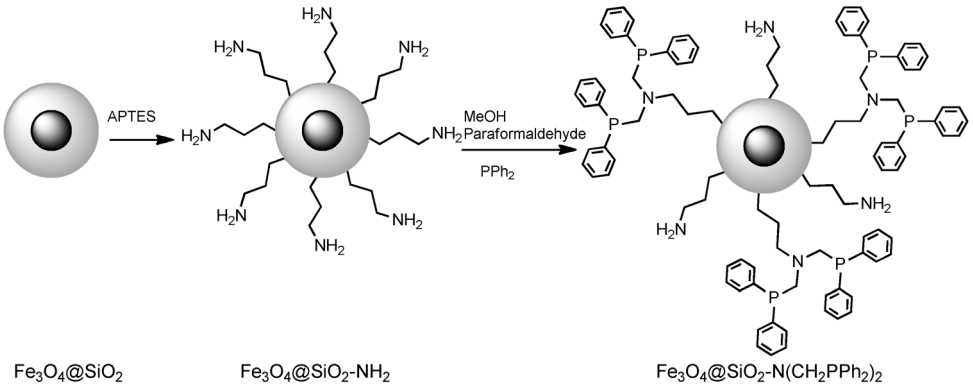

Scheme 2. Preparation steps for the Fe_3O_4@SiO_2-$N(CH_2PPh_2)_2$ support. APTES = (3-aminopropyl)triethoxysilane.

so-called phosphinomethylation reaction was expected to provide a double substitution in each terminal primary amino group.

The amino terminal groups grafted on the NP surface were quantified by thermogravimetric analysis. The mass loss attributed to the thermal decomposition of the chemically bonded aminopropyl ligands was 0.42 mg g^{-1}, which corresponded to 0.66 wt% of nitrogen or 0.5 mmol of $-NH_2$ per gram of the support. The amount of nitrogen in the material determined from elemental analysis was 0.64 wt%; this result was in agreement with the results obtained by thermogravimetric analysis.

The next step consisted in the phosphinomethylation of the amino terminal groups to produce propylamino bis(methylenediphenylphosphine) moieties [Fe_3O_4@SiO_2-$N(CH_2PPh_2)_2$]. The percentage of phosphorus in the material determined from the ICP–OES analysis was 0.94 wt%, which corresponded to 0.4 mmol of $-CH_2PPh_2$ per gram of the solid material. This value indicates that the phosphinomethylation reaction did not occur in all the amino groups available.

After the impregnation of Rh-TOAB NPs on the phosphine-functionalized solid, the percentage of rhodium determined from flame atomic absorption spectroscopy (FAAS) analysis was 0.2 wt%, which corresponded to a phosphorus/rhodium ratio of 16. The low loading of metal in the material did not allow the characterization of the supported catalyst by XRD and X-ray photoelectron spectroscopy; however, the supported rhodium NPs could be visualized by TEM. The presence of rhodium NPs on the surface of the material and the core–shell morphology of the support comprising magnetite NPs spherically coated by silica are revealed by Figure 1. The composition of rhodium NPs was confirmed by energy-dispersive X-ray spectroscopy analysis. Even though the FAAS analysis of the catalyst after the reaction (spent catalyst) revealed that the rhodium content was preserved (0.2 wt%), no rhodium NPs could be found on the support surface by TEM analysis.

The data on the hydroformylation of **1a** in the presence of Fe_3O_4@SiO_2-$N(CH_2PPh_2)_2$Rh are given in Table 2. The reaction at 60 °C occurred with high selectivity towards aldehydes **1b** and **1c** (96%), albeit at a relatively low rate, which resulted in 35% conversion in 24 h (Table 2, run 1). At 120 °C, a complete conversion was attained in 6 h; however, the hydroformylation selectivity decreased to 60% owing to the extensive substrate isomerization, which was responsible for 40% of the mass balance (Table 2, run 2). Thus, further tests were performed at a compromise temperature of 80 °C, which enabled the contribution of isomerization under 20% to be maintained at a reasonably high hydroformylation rate (Table 2, runs 3–8). The reactions were completed in approximately 6 h at a substrate-to-rhodium ratio of 2000 (Table 2, runs 3 and 8). Notably, aldehydes **1b** and **1c** were the only hydroformylation products and no aldehydes derived from the isomers of **1a** were detected. In addition, the Fe_3O_4@SiO_2-$N(CH_2PPh_2)_2$Rh material did not promote the hydrogenation of either the substrate or the aldehydes. The ratio between the linear and branched aldehydes in

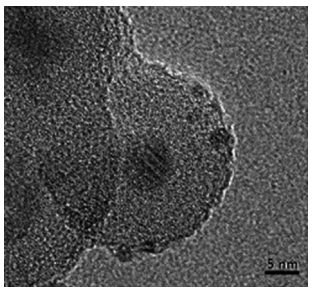

Figure 1. TEM image of the Fe_3O_4@SiO_2-$N(CH_2PPh_2)_2$Rh catalyst. Scale bar = 5 nm.

Table 2. Hydroformylation of **1a** catalyzed by Fe_3O_4@SiO_2-$N(CH_2PPh_2)_2$Rh.[a]

Run	Reaction cycle	T [°C]	t [h]	Conversion [%]	Selectivity [%]	
					Aldehydes (**1b**/**1c**)	Octene isomers
1	1	60	24	35	96 (2.31)	4
2	1	120	4	100	60 (2.48)	40
3	1	80	4	64	82 (2.28)	18
			6	96	82 (2.28)	18
4[b]	2	80	4	62	81 (2.24)	19
5[b]	3	80	4	67	84 (2.36)	16
6[b]	4	80	4	66	84 (2.36)	16
7[b]	5	80	4	67	86 (2.44)	14
8[b]	6	80	4	67	86 (2.44)	14
			6	100	81 (2.20)	19
9[c]	–	80	6	0	–	–

[a] Reaction conditions: **1a** (2 mmol), catalyst (50 mg, 1 μmol of Rh), toluene (10 mL), P = 60 atm (CO/H_2 = 1); conversion and selectivity were determined from GC analysis; the linear to branched ratio was given in parenthesis; [b] The spent catalyst recycled after run 3 was consequently used in these runs; [c] After run 3, the catalyst was magnetically removed (and was used in recycling experiments), fresh **1a** (2 mmol) added, and the reaction allowed to proceed; no further conversion was observed.

all runs was approximately 2.2–2.5; that is, the linear isomer responded for 70–85% of the aldehyde product, regardless of the reaction temperature. The Fe_3O_4@SiO_2-$N(CH_2PPh_2)_2Rh$ catalyst was also active for the hydroformylation of styrene (**2a**; Table 3). The selectivity towards the hydroformylation products aldehydes **2b** and **2c** was almost 100% in all runs. The catalyst promoted no hydrogenation under hydroformylation conditions, and the **2a** molecule had no option for isomerization.

Table 3. Hydroformylation of **2a** catalyzed by Fe_3O_4@SiO_2-$N(CH_2PPh_2)_2Rh$.[a]

Run	T [°C]	Conversion [%]	Selectivity [%]	
			2b	**2c**
1	80	5	23	75
2	100	70	25	73
3	120	90	52	47

[a] Reaction conditions: **2a** (2 mmol); catalyst (50 mg, 1 μmol of Rh); toluene (10 mL); $P=60$ atm ($CO/H_2=1$), $t=6$ h; conversion and selectivity were determined from GC analysis.

The kinetic curve for the first reaction using the Fe_3O_4@SiO_2-$N(CH_2PPh_2)_2Rh$ catalyst showed a clearly pronounced induction period of 1–2 h during which active catalytic species were likely formed from the rhodium precursor (Figure 2). According to Shylesh et al.,[6f] rhodium NPs can undergo corrosive chemisorption in the presence of carbon monoxide under hydroformylation conditions, which leads to a weakening of Rh–Rh bonds owing to the higher strength of Rh–CO bonds. This may suggest that molecular rhodium species are formed in situ, residing on the support due to the interactions with the phosphine ligands grafted on the silica matrix. The Fe_3O_4@SiO_2-$N(CH_2PPh_2)_2Rh$ catalyst was tested in recycling runs without interruptions to take aliquots for intermediate GC analyses. A reaction time of 4 h was chosen for each recycling run rather than the time necessary for complete conversion to avoid the camouflage of catalytic activity loss. The Fe_3O_4@SiO_2-$N(CH_2PPh_2)_2Rh$ material was magnetically recovered and used in six consecutive reactions, which showed the same catalytic performance without any loss in activity and selectivity (Table 2, runs 3–8). The reaction solutions after all runs listed in Table 2 contained no rhodium, as demonstrated by using ICP–OES analysis, considering the detection limit of the equipment. Moreover, after catalyst removal in run 3 for use in recycling experiments, a portion of fresh **1a** was added to the supernatant and the reaction was allowed to proceed; no further conversion was observed (Table 2, run 9). It is important to mention the high air stability of the catalyst, which was exposed to air during each recovering procedure in the recycling experiments and did not deactivate. In contrast, it should also be mentioned that the stability of the phosphine ligand requires more detailed studies. In principle, the surface diphenylphosphine ligand can undergo partial oxidation and be reduced again with hydrogen under reaction conditions. Alternatively, the effect of gradual oxidation of the immobilized ligand on the catalytic performance may remain unnoticed during six reaction cycles. Unfortunately, we could not reveal these processes detecting phosphine oxides by using IR spectroscopy owing to relatively low ligand concentration on the surface and strong adsorption of the silica support. Valuable information about ligand oxidation was obtained by using Raman spectroscopy (see below).

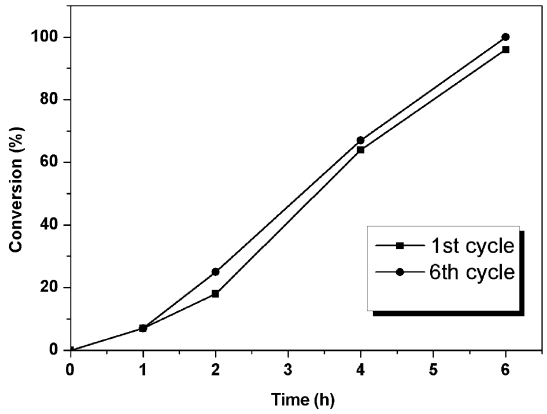

Figure 2. Hydroformylation of **1a** catalyzed by Fe_3O_4@SiO_2-$N(CH_2PPh_2)_2Rh$. Reaction conditions: **1a** (2 mmol), catalyst (50 mg, 1 μmol of Rh), toluene (10 mL), $P=60$ atm ($CO/H_2=1$), $T=80$ °C.

Monitoring of the sixth reaction cycle by using GC revealed that the kinetic curve was similar to that in the first reaction cycle, which also showed an induction period of approximately 1 h (Table 2, run 8; Figure 2). However, these induction periods may have arisen owing to distinct processes of the formation of catalytically active species. In the first run, it may have been related to the corrosive chemisorption of rhodium NPs; however, in the sixth run, other activation mechanisms should have been involved instead. As mentioned above, the TEM image of the freshly prepared Fe_3O_4@SiO_2-$N(CH_2PPh_2)_2Rh$ material revealed the presence of rhodium NPs on the surface. Conversely, the TEM analyses of the spent catalysts (both after the first use and after the sixth use) showed only the support, but not the rhodium NPs. Considering that the percentage of rhodium in spent catalysts was maintained and the fact that the catalyst was still active in the successive hydroformylation reactions, it is plausible to suggest that the corrosive chemisorption occurred on our Fe_3O_4@SiO_2-$N(CH_2PPh_2)_2Rh$ material in the first run and the phosphine ligands could anchor rhodium to the support surface. The activation mechanism in the sixth reaction may involve ligand reduction and should be further studied for clarification.

Unfortunately, the low metal loading (0.2 wt% rhodium) did not allow any XRD or X-ray photoelectron spectroscopic measurements to be recorded, which hindered the determination of the oxidation state of rhodium in the spent catalysts. We also failed to record FTIR spectra of the ligands and rhodium complexes which could exist on the support surface. However, we could shed some light on the interaction of the rhodium NPs and the diphenylphosphine ligand grafted on the support sur-

face by using Raman spectroscopy. Raman scattering becomes a sensitive and selective technique if associated with enhancement processes such as in resonance Raman (RR) spectroscopy and surface-enhanced Raman spectroscopy (SERS),[20] which provides useful information about the interaction between organic ligands and metals, including the coordination of functional groups with metal ions and metal surfaces.

The normal Raman spectrum of the air-sensitive ligand $HPPh_2$ obtained in a sealed tube under an inert atmosphere (Figure 3a) was dominated by the bands at 618 cm^{-1} (phenyl ring in-plane deformation), 683 cm^{-1} (phenyl ring out-of-plane deformation), 801 cm^{-1} (phenyl C–H out-of-plane deformation), 997 cm^{-1} (phenyl ring breathing), 1101 cm^{-1} (P–C ring stretching), and 1584 cm^{-1} (phenyl C–C stretching). We also recorded the normal Raman spectrum of the ligand after exposure to air. A new band at 1183 cm^{-1} can be attributed to the P=O stretching mode.[21] The Raman spectrum obtained from the diphenylphosphine ligand grafted on the support surface is shown in Figure 3c. In this case, the characteristic Raman bands of the ligand did not appear, most probably owing to its low concentration in the silica matrix. However, after impregnation with Rh-TOAB NPs, the characteristic bands of the ligand were revealed (Figure 3d), which suggests an enhancement of the Raman cross section of the ligand grafted on the silica matrix.

The Raman spectrum obtained after the immobilization of Rh-TAOB NPs on Fe_3O_4@SiO_2-$N(CH_2PPh_2)_2$ (Figure 3d) displays wavenumber shifts and an intensity pattern change as compared with the free phosphine spectra (Figure 3a and b). Notably, the changes in the Raman spectrum of the diphenylphosphine ligand upon interaction with Rh-TOAB NPs were similar to those reported by Hu et al.[22] for the interaction of PPh_3 with silver NPs. In both cases, the adsorption of a phosphine moiety on the metallic NP is characterized by the enhancement of the phenyl X-sensitive mode at approximately 521 cm^{-1}, the enhancement of the bands at 787 cm^{-1} assigned to the phenyl C–H out-of-plane deformation, and an upshift of the ring breathing mode located at approximately 1000 cm^{-1}. These changes, which are related to the electronic density of the phenyl rings, are analogous to those observed in the SERS spectrum of the PPh_3–Ag NP system. In contrast to the SERS spectrum, we could not observe the same enhancement of the P–C stretching vibration mode at 1101 cm^{-1}, which may suggest a different enhancement mechanism. The band at 1212 cm^{-1} may be assigned to the P=O stretching mode, which was upshifted with respect to the free ligand (1183 cm^{-1}), and suggested at least partial oxidation of the ligand grafted on the support surface.

If the Raman spectrum is obtained by using a radiation with similar energy of an electronic transition, the spectrum may be enhanced by several orders of magnitude owing to an RR effect.[20] To assign the enhancement of the Raman spectrum of the phosphine ligand observed after impregnation with Rh-TOAB NPs, the reflectance spectra of the material with and without rhodium NPs were investigated (Figure 4). Although the catalyst support (silica-coated iron oxide) itself absorbs significantly in the visible range, this absorption was strongly enhanced after the impregnation with Rh-TOAB NPs. The transition in the 500–800 nm region can be attributed to a charge transfer between the phosphine ligand and the metallic NP, as observed previously in similar systems.[22] The PPh_3–Ag NP system shows a transition centered at 706 nm, which was attributed to a charge transfer between PPh_3 and the silver surface. The presence of a charge transfer transition in the energy of the laser excitation used for the Raman measurements ($\lambda_{excitation}$ = 632.8 nm) provided a condition for RR scattering,

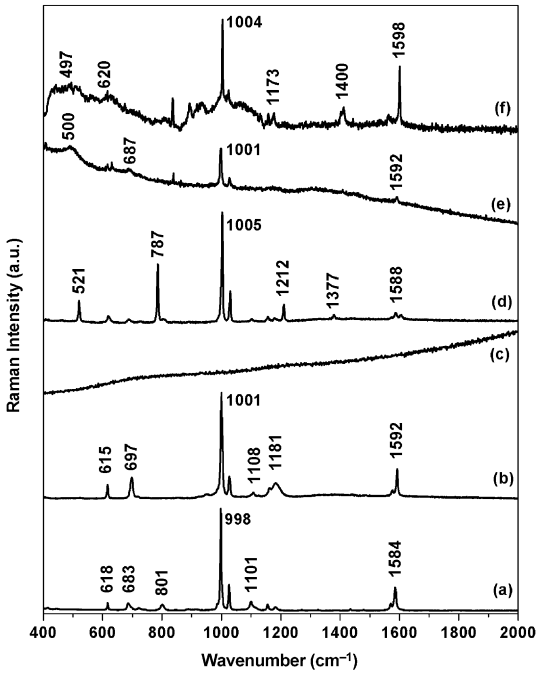

Figure 3. Raman spectra of a) diphenylphosphine, b) diphenylphosphine oxide, c) Fe_3O_4@SiO_2-$N(CH_2PPh_2)_2$, d) Fe_3O_4@SiO_2-$N(CH_2PPh_2)_2Rh$ catalyst, e) Fe_3O_4@SiO_2-$N(CH_2PPh_2)_2Rh$ catalyst after the reaction (spent catalyst), and f) material prepared by the interaction of Rh^{3+} and Fe_3O_4@SiO_2-$N(CH_2PPh_2)_2$. Data were collected at $\lambda_{excitation}$ = 632.8 nm.

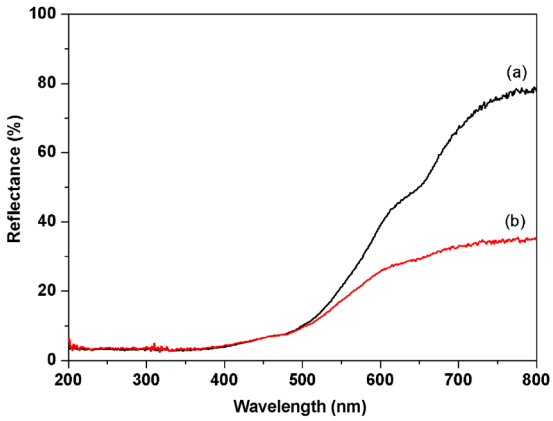

Figure 4. Reflectance spectra of a) Fe_3O_4@SiO_2 and b) Fe_3O_4@SiO_2-$N(CH_2PPh_2)_2Rh$.

which enabled the observation of the diphenylphosphine vibrational modes in Figure 3d. The RR spectrum agrees well with the SERS spectrum of the PPh_3–Ag NP system previously reported in the literature.[22]

Raman scattering was also used to investigate the spent catalyst recovered after the hydroformylation reaction. The Raman spectrum shown in Figure 3e exhibits many changes compared with that of the as-prepared catalyst shown in Figure 3d. The band assigned to the P=O stretching mode at 1212 cm^{-1} is absent, which is an evidence that diphenylphosphine oxide was reduced under reaction conditions; however, the stability of the phosphorus ligand requires more detailed studies. Although the main bands attributed to the phosphine ligand are still observed (1001, 1028, and 1592 cm^{-1}), the bands previously assigned to an enhancement by the interaction with the metal NP surface (521 and 787 cm^{-1}) are absent. This observation provides additional evidence for a corrosive chemisorption of rhodium NPs under hydroformylation conditions, which would lead to the formation of a molecular rhodium complex still attached to the support owing to the interaction with the phosphine ligand grafted on the silica matrix. For comparison, a rhodium complex was prepared by reacting the Fe_3O_4@SiO_2-$N(CH_2PPh_2)_2$ support with Rh^{3+} ions. The Raman spectrum of the supported rhodium complex (Figure 3f) revealed similarities with the spectrum of the spent catalyst (Figure 3e), which corroborates the role of Rh-TOAB NPs as precursors for the formation of a rhodium–phosphine complex on the support surface under catalytic reaction conditions.

Conclusions

The immobilization of rhodium nanoparticles (NPs) stabilized by tetraoctylammonium bromide (Rh-TOAB NPs) on a magnetic support with diphenylphosphine ligands grafted on its surface enabled the preparation of an air-stable, easily recoverable, and reusable catalyst for the hydroformylation of olefins. We observed a strong interaction between the rhodium NPs and the phosphine ligands grafted on the support surface, which caused an enhancement in the Raman spectrum of the ligand. Analysis of the recovered catalyst after the hydroformylation reaction reveals that such interaction is no longer present, which indicates the dissolution of rhodium NPs and formation of molecular rhodium species. These active species are formed in situ and maintained on the magnetic support surface after magnetic separation. The results of Raman spectroscopy also indicate the oxidation of the diphenylphosphine ligand grafted on the silica matrix after exposure to air and its possible reduction under reaction conditions. Recycling studies show negligible metal leaching and high activity, which are maintained in successive reactions. It is important to mention that both the Rh-TOAB NPs and the supported Fe_3O_4@SiO_2-$N(CH_2PPh_2)_2Rh$ catalyst are stable in air and can be exposed to air during the preparation steps and work-up procedures in recycling studies. This is a special feature of our catalyst and a distinct behavior as compared with many air-sensitive homogeneous and heterogeneous catalyst counterparts.

Experimental Section

Preparation of rhodium NPs

Rhodium NPs were synthesized by using the modified method described by Brust et al.[13] Rhodium(III) chloride hydrate (30 mg, 0.11 mmol of Rh) and TOAB (130 mg, 0.23 mmol) were dissolved in deionized water (30 mL) and toluene (30 mL), respectively, at RT. The aqueous phase was adjusted to pH 6 by the addition of aqueous NaOH. The phase transfer reagent solution was added dropwise to the Rh^{3+} aqueous solution, and the mixture was stirred for 30 min. An aqueous sodium borohydride solution (5 mL, 1.36 mmol) was freshly prepared and added dropwise to the mixture. The organic layer turned black, and the system was further stirred for 3 h. Then, the organic phase containing rhodium NPs was separated and washed twice with water. The NPs synthesized using this procedure were labelled as Rh-TOAB NPs.

Preparation of the catalyst support

The catalyst support consists of silica-coated magnetite NPs (Fe_3O_4@SiO_2) prepared following the procedure described elsewhere.[14] The solid was calcined for 2 h at 540 °C, and then the silica surface was modified with terminal amino groups using (3-aminopropyl)triethoxysilane. The solid (200 mg) was added to the (3-aminopropyl)triethoxysilane solution (1% v/v) in dry toluene (200 mL) under N_2 atmosphere. The mixture was stirred at RT for 2 h, and then the solid was separated magnetically. The material, labelled as Fe_3O_4@SiO_2-NH_2, was washed twice with toluene and acetone and dried at 100 °C for 20 h.

In the next step, terminal amino groups in Fe_3O_4@SiO_2-NH_2 were subjected to phosphinomethylation.[15] Under an inert atmosphere, the mixture of paraformaldehyde (1.82 mmol) and diphenylphosphine (2.00 mmol) in methanol (5 mL) was heated at 60 °C for 1 h. Then, the suspension of Fe_3O_4@SiO_2-NH_2 (1.00 g, 0.5 mmol of NH_2) in a toluene (20 mL)–methanol (10 mL) solution was added to the reaction mixture, which was stirred overnight at RT (25 °C). Then, the solid, labelled as Fe_3O_4@SiO_2-$N(CH_2PPh_2)_2$, was washed five times with toluene and dried under vacuum. Both Fe_3O_4@SiO_2-NH_2 and Fe_3O_4@SiO_2-$N(CH_2PPh_2)_2$ materials were further used as supports for the immobilization of rhodium NPs.

Preparation of supported rhodium NP catalysts

A toluene solution containing Rh-TOAB NPs (≈30 mL, 0.11 mmol of Rh) was added to the Fe_3O_4@SiO_2-NH_2 or Fe_3O_4@SiO_2-$N(CH_2PPh_2)_2$ support (500 mg). The mixtures were stirred overnight, and then the solids were separated magnetically. After the separation, the catalysts were washed several times with toluene and dried under vacuum. The materials obtained are labelled as Fe_3O_4@SiO_2-NH_2Rh and Fe_3O_4@SiO_2-$N(CH_2PPh_2)_2Rh$, respectively. The ICP–OES analysis showed that the rhodium content was 0.7 wt% in Fe_3O_4@SiO_2-NH_2Rh and 0.2 wt% in Fe_3O_4@SiO_2-$N(CH_2PPh_2)_2Rh$.

Catalytic reactions

The hydroformylation reactions were performed in a home-made 100 mL stainless steel reactor. In a typical run, the mixture of toluene (10 mL), the rhodium catalyst (50 mg, 1.0–3.4 μmol of Rh), **1a** or **2a** (2.0 mmol), and dodecane (internal standard, 1 mmol) was transferred to the reactor, which was pressurized to 60 atm

($CO/H_2 = 1$; 1 atm = 101.3 kPa). The temperature was maintained with an oil bath and a hot stirring plate connected to a digital temperature controller. The reactions were performed under magnetic stirring (700 rpm). After the completion of the reaction, the reactor was cooled to RT, the pressure was released, and the catalyst was recovered magnetically with an external magnet. The reaction solution was analyzed by using GC. Toluene was purified under reflux with sodium wire–benzophenone for 8 h and then distilled under argon atmosphere.

Methods

TEM analysis was performed with a JEOL 2100 microscope. Samples for TEM were prepared by placing a drop of NPs dispersed in propan-2-ol on a carbon-coated copper grid (Ted Pella, Inc.). The rhodium content in all catalysts was measured by using FAAS with a Shimadzu AA-6300 atomic absorption spectrophotometer. The rhodium leaching into the supernatant solutions was measured with a SPECTRO ARCOS ICP–OES spectrometer. The products were analyzed by using GC (Shimadzu QP2010 instrument equipped with an Rtx-5MS capillary column and a flame ionization detector) and GC–MS (Shimadzu QP2010-Plus instrument operating at 70 eV). Conversion and selectivity were determined from GC analysis. The GC mass balance was based on the substrate charged using dodecane as an internal standard. The Raman spectra were recorded on a Renishaw inVia Raman microscope equipped with a charge-coupled device detector and coupled to a Leica optical microscope, which enabled rapid accumulation of the Raman spectra with a spatial resolution of approximately 1 mm (micro-Raman technique). The laser beam was focused on the sample with a 50× lens. Laser power was always kept below 0.7 mW at the sample. The experiments were performed under ambient conditions by using a backscattering geometry. The samples were irradiated with the 632.8 nm line of a He–Ne laser (Renishaw RL633 laser).

Acknowledgements

We are grateful to INCT-Catálise and the Brazilian government agencies FAPESP, CNPq, and FAPEMIG for financial support.

Keywords: diphenylphosphine · hydroformylation · nanoparticles · Raman spectroscopy · rhodium

[1] R. Franke, D. Selent, A. Börner, *Chem. Rev.* **2012**, *112*, 5675 – 5732.
[2] a) E. V. Gusevskaya, J. Jiménez-Pinto, A. Börner, *ChemCatChem* **2014**, *6*, 382 – 411; b) G. Whiteker, C. Cobley, in *Organometallics as Catalysts in the Fine Chemical Industry* (Eds.: M. Beller, H.-U. Blaser), Springer Berlin – Heidelberg, **2012**, pp. 35 – 46.
[3] C. D. Frohning, C. W. Kohlpaintner, H.-W. Bohnen, in *Applied Homogeneous Catalysis with Organometallic Compounds* (Eds.: B. Cornyls, W. A. Herrmann), Wiley-VCH, Weinheim, **2008**, pp. 29 – 194.
[4] P. N. M. van Leeuwen, C. Casey, G. Whiteker in *Rhodium-Catalyzed Hydroformylation* (Eds.: P. N. M. Van Leeuwen, C. Claver), Springer, Netherlands, **2002**, pp. 63 – 105.
[5] a) V. A. Likholobov, B. L. Moroz, in *Handbook of Heterogeneous Catalysis* (Eds.: G. Ertl, H. Knözinger, J. Weitkamp), Wiley-VCH, Weinheim, **2008**, pp. 2231 – 2334; b) L. Obrecht, P. C. J. Kamer, W. Laan, *Catal. Sci. Technol.* **2013**, *3*, 541 – 551; c) X. Li, Y. Ding, G. Jiao, J. Li, L. Ya, H. Zhu, *J. Nat. Gas Chem.* **2008**, *17*, 351 – 354; d) X. Li, Y. Ding, G. Jiao, J. Li, R. Lin, L. Gong, L. Yan, H. Zhu, *Appl. Catal. A* **2009**, *353*, 266 – 270; e) A. C. B. Neves, M. J. F. Calvete, T. M. V. D. Pinho e Melo, M. M. Pereira, *Eur. J. Org. Chem.* **2012**, 6309 – 6320; f) T. T. Adint, C. R. Landis, *J. Am. Chem. Soc.* **2014**, *136*, 7943 – 4953.
[6] a) A. J. Bruss, M. A. Gelesky, G. Machado, J. Dupont, *J. Mol. Catal. A* **2006**, *252*, 212 – 218; b) M. R. Axet, S. Castillón, C. Claver, K. Philippot, P. Lecante, B. Chaudret, *Eur. J. Inorg. Chem.* **2008**, 3460 – 3466; c) J. Kim, J. Park, O.-S. Jung, Y. Chung, K. Park, *Catal. Lett.* **2009**, *128*, 483 – 486; d) A. Behr, Y. Brunsch, A. Lux, *Tetrahedron Lett.* **2012**, *53*, 2680 – 2683; e) R. Amrousse, K. Hori, W. Fetimi, *Catal. Commun.* **2012**, *27*, 174 – 178; f) S. Shylesh, D. Hanna, A. Mlinar, X.-Q. n. Kŏng, J. A. Reimer, A. T. Bell, *ACS Catal.* **2013**, *3*, 348 – 357.
[7] a) M. Nandi, P. Mondal, M. Islam, A. Bhaumik, *Eur. J. Inorg. Chem.* **2011**, 221 – 227; b) N. Sudheesh, A. K. Chaturvedi, R. S. Shukla, *Appl. Catal. A* **2011**, *409*, 99 – 105.
[8] a) V. K. Srivastava, S. K. Sharma, R. S. Shukla, R. V. Jasra, *Ind. Eng. Chem. Res.* **2008**, *47*, 3795 – 3803; b) S. K. Sharma, P. A. Parikh, R. V. Jasra, *J. Mol. Catal. A* **2010**, *316*, 153 – 162.
[9] a) B. Li, X. Li, K. Asami, K. Fujimoto, *Chem. Lett.* **2003**, *32*, 378 – 379; b) Y. Zhang, M. Shinoda, Y. Shiki, N. Tsubaki, *Fuel* **2006**, *85*, 1194 – 1200.
[10] a) L. Oresmaa, M. A. Moreno, M. Jakonen, S. Suvanto, M. Haukka, *Appl. Catal. A* **2009**, *353*, 113 – 116; b) M.-L. Kontkanen, L. Vlasova, S. Suvanto, M. Haukka, *Appl. Catal. A* **2011**, *401*, 141 – 146; c) R. Chansarkar, A. A. Kelkar, R. V. Chaudhari, *Ind. Eng. Chem. Res.* **2009**, *48*, 9479 – 9489.
[11] D. Han, X. Li, H. Zhang, Z. Liu, G. Hu, C. Li, *J. Mol. Catal. A* **2008**, *283*, 15 – 22.
[12] S. E. Lyubimov, E. A. Rastorguev, K. I. Lubentsova, A. A. Korlyukov, V. A. Davankov, *Tetrahedron Lett.* **2013**, *54*, 1116 – 1119.
[13] M. Brust, M. Walker, D. Bethell, D. J. Schiffrin, R. Whyman, *Chem. Commun.* **1994**, 801 – 802.
[14] M. J. Jacinto, P. K. Kiyohara, S. H. Masunaga, R. F. Jardim, L. M. Rossi, *Appl. Catal. A* **2008**, *338*, 52 – 57.
[15] M. T. Reetz, G. Lohmer, R. Schwickardi, *Angew. Chem. Int. Ed. Engl.* **1997**, *36*, 1526 – 1529; *Angew. Chem.* **1997**, *109*, 1559 – 1562.
[16] L. Rossi, L. R. Vono, M. S. Garcia, T. T. Faria, J. Lopez-Sanchez, *Top. Catal.* **2013**, *56*, 1228 – 1238.
[17] L. M. Rossi, M. A. S. Garcia, L. L. R. Vono, *J. Braz. Chem. Soc.* **2012**, *23*, 1959 – 1971.
[18] M. J. Jacinto, F. P. Silva, P. K. Kiyohara, R. Landers, L. M. Rossi, *ChemCatChem* **2012**, *4*, 698 – 703.
[19] a) N. J. S. Costa, L. M. Rossi, *Nanoscale* **2012**, *4*, 5826 – 5834; b) T. A. G. Silva, R. Landers, L. M. Rossi, *Catal. Sci. Technol.* **2013**, *3*, 2993 – 2999.
[20] H. Kim, K. M. Kosuda, R. P. Van Duyne, P. C. Stair, *Chem. Soc. Rev.* **2010**, *39*, 4820 – 4844.
[21] G. B. Deacon, J. H. S. Green, *Spectrochim. Acta* **1968**, *24A*, 845 – 852.
[22] G. Hu, Z. Feng, D. Han, J. Li, G. Jia, J. Shi, C. Li, *J. Phys. Chem. C* **2007**, *111*, 8632 – 8637.

Received: January 23, 2015
Revised: March 5, 2015
Published online on May 4, 2015